Available online at www.sciencedirect.com
ScienceDirect
Ceramics International 37 (2011) 2007–2014
CERAMICS INTERNATIONAL
www.elsevier.com/locate/ceramint

Synthesis and solubility of calcium fluoride/hydroxy-fluorapatite nanocrystals for dental applications

Mahmoud Azami [a,b,*], Sasan Jalilifiroozinezhad [a], Masoud Mozafari [a], Mohammad Rabiee [a]

[a] Biomaterials Group, Faculty of Biomedical Engineering (Center of Excellence), Amirkabir University of Technology, P. O. Box: 15875-4413, Tehran, Iran
[b] Tissue Engineering and Cell Therapy Department, School of Advanced Medical Technologies, Tehran University of Medical Sciences, Tehran, Iran

Received 23 November 2010; received in revised form 16 December 2010; accepted 26 February 2011
Available online 8 April 2011

Abstract

As the mineral phase of tooth enamel consists of apatite containing fluoride, the ''CaF_2-like'' salts are of significant interest in dentistry for their roles as labile fluoride reservoirs in caries prevention. Fluoride ion is required for normal dental development because of its therapeutic ability of osteoporosis healing and stimulating osteoblast activity both *in vitro* and *in vivo*. In this research, biphasic Calcium fluoride/fluorinated-hydroxyapatite (CF/FHAp) nanocrystals have been successfully synthesized via co-precipitation method. The synthesized powder was characterized by the commonly used bulk techniques such as chemical analysis, Fourier transform infrared spectroscopy (FTIR), scanning electron microscopy (SEM), energy dispersive spectroscopy (EDS) and X-ray powder diffraction (XRD) analyses. The obtained results confirmed the formation of biphasic powder composed of about 46% CF and 54% (w/w%) apatite phase which was a solid solution composed of more than 50% fluorapatite (FAp). In addition, *in vitro* evaluations of the powder were performed, and for investigating their bioactive capacity they were soaked in simulated body fluid (SBF) at different time intervals. The samples showed significant enhancement in bioactivity within few hours of immersion in SBF solution. Also, the EDS analysis clearly showed dissolution and deposition of calcium and phosphate ions on the surface of synthesized biphasic powder after the first week of immersion in SBF solution.

Keywords: Calcium fluoride; Fluorinated-hydroxyapatite; Solid solution; Co-precipitation method; *in vitro* evaluation; Dental applications

1. Introduction

Synthetic hydroxyapatite (HAp) has been used extensively as a bone implant material due to its identical chemical composition and high biocompatibility with natural bone [1–3]. The inorganic matrix component of natural bone is based on HAp with formulation of $Ca_{10}(PO_4)_6(OH)_2$ doped with different quantities of cations like Na^+, K^+ and Mg^{2+} which occupy Ca^{2+} sites and anions such as CO_2^{3-}, SO_2^{4-} and F^- substituting OH^- groups. According to the previous studies, these dopants especially F^- have a great influence on the physical and biological properties of the material [4,5]. There are also various FHAps with different degrees of fluorination, $Ca_{10}(PO_4)_6(OH)_{2-2x}F_{2x}$ (x is the degree of fluorination, $x = 0$ HAp, $x = 1.0$ FAp, $0 < x < 1$ forms FHAp solid solution). Fluorine tends to reduce the crystal size and increases stability of the apatite structure. At lower degrees of fluoridation the apparent solubility declines markedly. It was suggested that FHAp has a better thermal and chemical stability than HAp [6]. This phenomenon which was described well by Elliott *et al.* [7] could be explained by considering the crystal structure of apatites. When a certain amount of F^- ions substituted with the OH^- groups in the HAp matrix, a certain level of chemical and thermal stability of the FHAp ceramics will be achieved. Theoretically, F^- ion concentration of 50% in the FHAp would be enough to remove the disorder of the crystal structure of HAp and hence stabilize its structure due to the alternating arrangement of the F^- ions between each pair of OH^- groups. However, by considering the random substitution of OH^- ions with F^- ions in the OH^- positions, the F^- ion concentration required for stabiling the structure was necessarily higher than 50% [1]. Thus, FHAp exhibits a considerable combination of stability and biocompatibility [6].

Additionally, fluoride is an essential trace element required for normal dental and skeletal development. It has been shown that the presence of fluoride posses beneficial effects on

* Corresponding author. Fax: +98 21 66468186.
E-mail address: mazami@aut.ac.ir (M. Azami).

0272-8842/$36.00
doi:10.1016/j.ceramint.2011.02.025

increasing the quantity and quality of bone formation in the body [8]. Thus, the bone mineral produced by FAp is less susceptible to dissolution and possible resorption. The fluoride ion has a therapeutic ability for healing of osteoporosis, since the bone mass is increased with F^- ion administration [9]. F^- ion is known to stimulate osteoblast activity both *in vitro* and *in vivo*. In addition, the mineral phase of tooth enamel consists of apatite containing 0.04 wt. % to 0.07 wt. % of fluoride, and constitutes about 95 to 97% of the dry mass. F^- ions present in saliva and blood plasma, are required for normal dental and skeletal development. It has been suggested that intaking fluoride of about 1.5–4 mg/day significantly reduces the risk of dental caries [10]. Owing to the fact that fluoride is well known for caries prevention and treatment of osteoporosis, FAp has been widely investigated [6,7,9–19].

CF and "CaF_2-like" materials are also of significant interest in dentistry due to their roles as labile fluoride reservoirs in caries prevention. Low concentration of F in oral fluids derived from labile F^- reservoirs formed by the use of F^- dentifrices and rinses has been shown to have profound effects on the progression of dental caries [20–22]. However, the low Ca concentration in the mouth provides a limited driving force for the formation of CaF_2, and only very small amounts of CaF_2-like deposits are formed after a conventional sodium fluoride rinse [23]. Precipitation of CaF_2 can cover the entire surface of hydroxyapatite when supplied at a sufficiently high concentration[24]. Previous studies showed that a two-solution delivery system, which supplies both F and Ca in a way that leads to homogeneous nucleation and formation of very small CaF_2 crystals in the mouth during application, was highly effective in increasing deposition and retention of labile F in the mouth [25,26]. This, in turn, increased the remineralization effects of the F regimen without increasing the F levels [27,28].

There are several methods of synthesizing HAp and FHAp with varied fluorine contents, such as, precipitation [29,30], sol-gel [31] a solid state reaction [32], and pyrolysis methods [33]. Also, CF powder was synthesized by different methods such as sol–gel method [34–36], solvothermal process [37,38], reverse micelle method [39,40], different precipitation methods [41–44], flame synthesis [45] and spray-drying process [46]. Among the methods mentioned above, precipitation method appears to be the most widely used for both FHAp and CF bioceramics.

The present study was aimed at preparing biphasic CF/FHAp solid solution through a continuous precipitation method especially for dental applications, which could be used not only as an osteoconductive material due to the nature of FHAp but also, as a labile F^- reservoir for developing potentially more effective F^- regimens and as an agent for use in the reduction of dentin permeability and dental caries prevention.

2. Materials and methods

2.1. Synthesis of biphasic powder

In a typical experiment, 0.03 M diammonium hydrogen phosphate solution [$(NH_4)_2HPO_4$, %99, Merck; No.1207], 0.05 M calcium nitrate 4-hydrate solution [$Ca(NO_3)_2$.$4H_2O$, %98, Merck PROLABO; No.22 384.298] and a mixed solution containing 0.03 M ammonia(NH_3, Merck; No. 1.05426) with 0.01 M ammonium fluoride(NH_4F, Merck; No. 101164) were prepared. The latter solution was a buffer solution in which its pH can be measured by the following equation (1):

$$\mathrm{pH} = 9.24 + Log\frac{[NH_3]}{[NH4^+]} \quad (1)$$

Therefore, the value of the obtained pH was 9.72. This buffer solution was used to simultaneously provide fluoride ion and also keeping pH at a constant value for synthesizing proper product. Required volume of buffer solution was added to both solutions to adjust their pH on 9.72. Afterward, phosphate solution was added drop-wise into calcium nitrate solution, at ambient temperature, resulting in the precipitation of a biphasic powder. During reaction, pH of the reactor was maintained on initial value by continuous adding of buffer solution. The precipitation of product can be described by simultaneous reactions leading to apatite phase. It could be HAp (Eq. 2) or FAp (Eq. 3) or the reaction which leads to CF (Eq. 4) as follow:

$$5Ca(NO_3)_2.4H_2O + 3(NH_4)_2HPO_4 + 4NH_4OH = Ca_5(PO_4)_3(OH) + 10NH_4NO_3 + 23H_2O \quad (2)$$

$$5Ca(NO_3)_2.4H_2O + 3(NH_4)_2HPO_4 + 3NH_4OH + 1NH_4F = Ca_5(PO_4)_3F + 10NH_4NO_3 + 23H_2O \quad (3)$$

$$Ca(NO_3)_2.4H2O + 2NH_4F = 1CaF_2 + 2NH_4NO_3 + 4H_2O \quad (4)$$

The precipitate was centrifuged and washed with de-ionized distilled water. The processes of centrifuging and washing were carried out twice. The obtained powder was dried in a lyophilizer system (Alpha 1–2LD, Germany) overnight. The schematic flowchart of the synthesis procedure is shown in Fig. 1.

2.2. Preparation of SBF solution

The SBF solution was prepared by dissolving reagent-grade NaCl, KCl, $NaHCO_3$, $MgCl_2.6H_2O$, $CaCl_2$ and KH_2PO_4 into distilled water and buffered at pH = 7.25 with TRIS (trishydroxymethyl aminomethane) and 1 M HCl solution at 37 °C. Therefore, concentration of Na^+, K^+, Mg^{2+}, Ca^{2+}, Cl^-, HCO^{3-}, HPO_4^{2-}, SO_4^{2-} ions in the prepared SBF solution was 142.0, 5.0, 1.5, 2.5, 147.8, 4.2, 1.0 and 0.5 mmol/dm^3, respectively. It should also be noted here that SBF is a solution highly supersaturated with respect to apatite [47].

2.3. Characterization

2.3.1. SEM observations

The microstructure of the prepared samples was examined by SEM. For this aim, the samples were coated with a thin layer of Gold (Au) by sputtering (EMITECH K450X, England) and then the microstructure and morphology of them were evaluated by SEM (Philips XL30) that operated at the acceleration voltage of 15 kV.

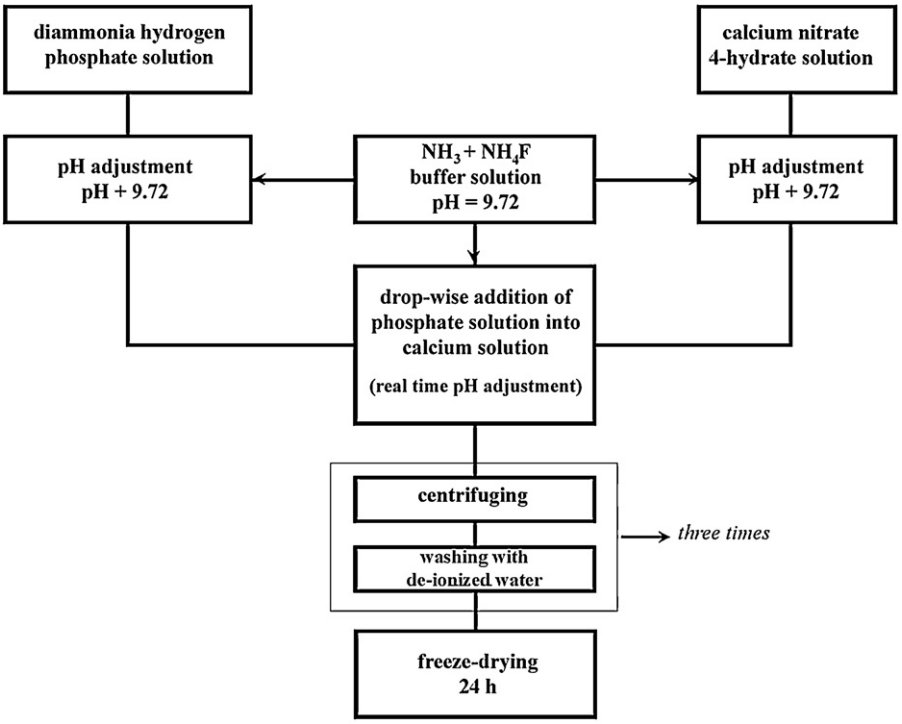

Fig. 1. The schematic flowchart of the synthesis procedure.

2.3.2. EDS analysis

EDS (Rontec, Germany) connected to SEM was used to investigate semi-quantitatively chemical compositions.

2.3.3. FTIR analysis

The synthesized samples were examined by Fourier transform infra-red spectroscopy with Bomem MB 100 spectrometer. For IR analysis, at first, 1 mg of the powder sample was carefully mixed with 300 mg of KBr (infrared grade) and pelletized under vacuum. Then the pellet was analyzed in the range of 500 to 4000 cm^{-1} at the scan speed of 23 scan/min with 4 cm^{-1} resolution.

2.3.4. XRD analysis

The obtained powder was analyzed by XRD with Siemens-Brucker D5000 diffractometer. This instrument works with voltage and current settings on 40 kV and 40 mA respectively and uses Cu-Kα radiation (1.540600 Å), and with the slit width of 1 mm. For qualitative analysis, XRD diagrams were recorded in the interval $20 \leq 2\theta \geq 70^{\circ}$ at scan speed of 2°/min being the step size 0.02° and the step time 1 s.

2.3.5. Microstructural evaluations

Crystallographic identification of the phases of synthesized powder was accomplished by comparing the experimental XRD patterns to standards be compiled by the International Center for Diffraction Data (ICDD), which was card #09-0432 for HA, #15-0876 for FA and # 77-2096 for CaF_2. The average size of the individual crystallites was calculated from XRD data using the Scherrer approximation (Eq. 5):

$$t = \frac{0.9\lambda}{\beta_{1/2}\cos\theta} \tag{5}$$

where t is the crystallite size, λ is the wavelength of Cu-Kα radiation (1.540560 Å) and $\beta_{1/2}$ is full width at half maximum intensity.

The lattice parameters such as a and c of synthesized powders was calculated by using the Eq. 6 for cubic and Eq. 7 and 8 for hexagonal systems, respectively, as follow:

$$\sin^2\theta = \frac{\lambda^2}{4a^2}(h^2 + k^2 + l^2) \quad \text{For } (h\,k\,l) \text{ plane} \tag{6}$$

$$\sin^2\theta = \frac{\lambda^2}{4}\left[\frac{4}{3}\frac{(h^2 + hk + k^2)}{a^2} + \frac{l^2}{c^2}\right] \quad \text{For } (h\,k\,l) \text{ plane} \tag{7}$$

$$\sin^2\theta = \frac{\lambda^2}{4}\left[\frac{4}{3}\frac{(h^2 + hk + k^2)}{a^2}\right] \quad \text{For } (h\,k\,0) \text{ plane} \tag{8}$$

2.3.6. Bulk elemental analysis

Fluorine and calcium contents of the precipitated powders were chemically analyzed by potentiometry and titration techniques, respectively [48]. This experiment was carried out to estimate the amount of each compound in the synthesized powder.

2.3.7. In vitro bioactivity study in SBF solution

For this aim, samples were soaked in SBF solution at 37 °C for 14 days. At regular intervals for 6 h and 1, 7, 14 days samples were taken out by centrifugation and rinsed with

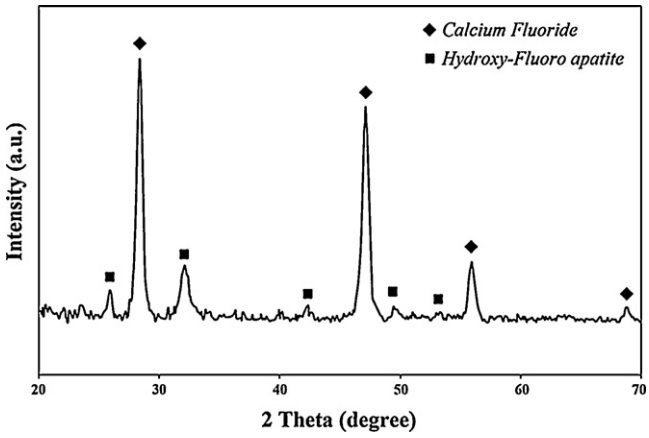

Fig. 2. XRD pattern of the synthesized apatite with CaF_2.

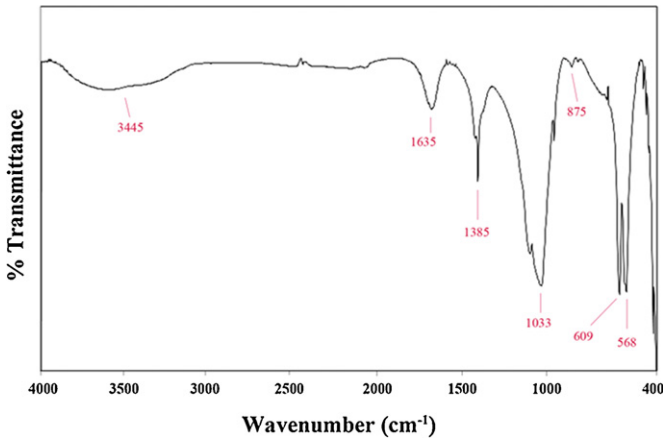

Fig. 3. FTIR spectrum of the synthesized calcium fluoride/hydroxy-fluorapatite powder.

doubly distilled water, and then dried with lyophilizer overnight.

2.4. Statistical analysis

All experiments were performed in five replicates. The results were given as means ± standard error (SE). Statistical analysis was performed by using One-way ANOVA and Tukey test with significance reported when $P < 0.05$. Also Kolmogorov-Smirnov test was used for investigation of group normalizing.

3. Results and discussion

3.1. XRD analysis

The XRD pattern of the synthesized sample is shown in Fig. 2. As it can be seen in this figure, the straight base line and the sharp peaks confirms that the product was well crystallized. The XRD pattern indicates that two distinct phases were formed in the obtained powder: apatite and CF. It is worth mentioning that all the peaks were concerned with these phases and trace of no other compound was detected by this technique.

To obtain more information from this pattern, the crystallographic parameters of observed phases were calculated, which are shown in Table 1 along with the same data for HAp, FAp and CF extracted from ICDD database. As it can be concluded from this table, the value of calculated unit cell parameter *a* for apatite phase in the synthesized sample was between pure FAp and HAp, while for parameter *c*, it was equal to all of them. Thus, it is evident that the synthesized apatite phase is a solid solution of FAp and HAp. On the other hand, some parts of hydroxyl groups in HAp have been substituted by fluoride ion and formed FHAp.

As it is shown in Table 1, the parameter *a* of CF phase in the synthesized sample was almost equal to indexed value for standard CF in database. According to Debye approximation, the crystallite sizes of FHAp and CF were 9.84 and 12.20 nm, respectively.

In continuous solid solutions of ionic salts, the lattice parameter of the solution is proportional to the atomic percent solute present. This relation is known as Vegard's law [49]. It could be concluded from this law that, substitution of OH^- locations in HAp crystal by other ions such as F^- and Cl^-, change lattice parameter linearly proportionate with the amount of substituted ions. Although, this law is not strictly obeyed by all types of apatite crystals [50,51], it can give an approximation to determine how much OH groups have been substituted by F^- ions in FHAp crystal structure. Rodriguez-Lorenzo *et al.* [30] investigated the influence of F^- ion on the structure of synthesized crystals and others have shown its influence on the mechanical properties [52], solubility [53], biocompatibil-

Table 1
Unit cell parameters of the synthesized powder in comparison with ICDD database.

Sample	a(A°)	c(A°)
HA (JCPDS # 09-0432)	9.42	6.88
FA (JCPDS #15-0876)	9.36	6.88
Apatite phase of the synthesized powder	9.39	6.88
CF (JCPDS # 77-2096)	5.44	———
CF phase of the synthesized powder	5.45	———

Table 2
Infrared assigned for the synthesized powder.

Infrared frequency (cm^{-1})	Assignment
568, 609	PO_4^{-3} bend ν_4
875, 1385, 1635	CO_3^{-2}
1033	PO_4^{-3} bend ν_3
3445	OH···F

Table 3
Weight percent of related elements in different compound in comparison with synthesized powder.

F(wt%)	Ca)wt%)	Compound
49	51	CF
–	39.8	HAp
3.76	39.6	FAp
24.32	40.48	Synthesized powder

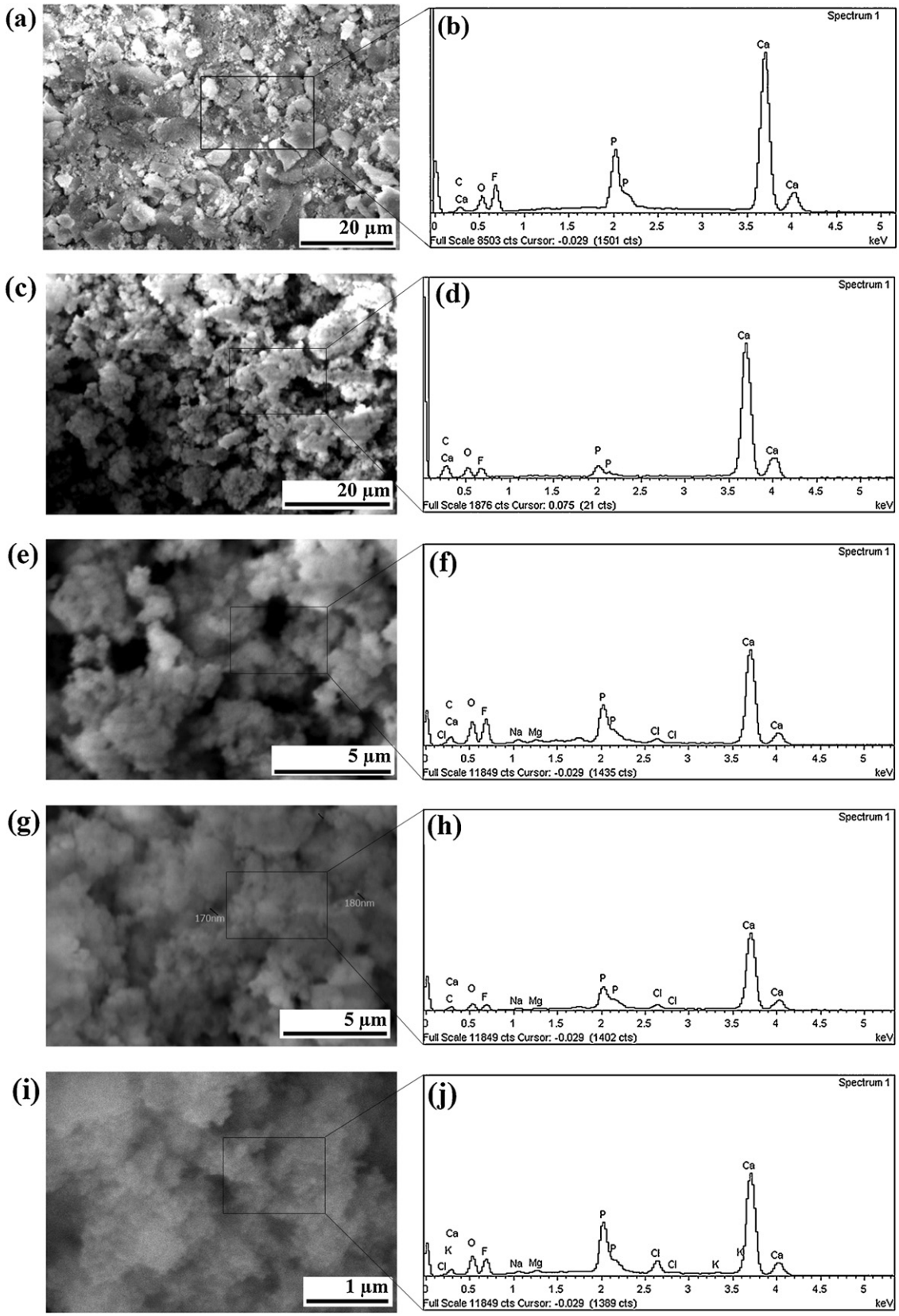

Fig. 4. SEM micrographs and EDS pattern of the synthesized powder before (a) and (b) and after soaking in SBF for various times, (a) and (b) 6 h, (c) and (d) 1 day, (e) and (f) 7 days, (g) and (h) 14 days.

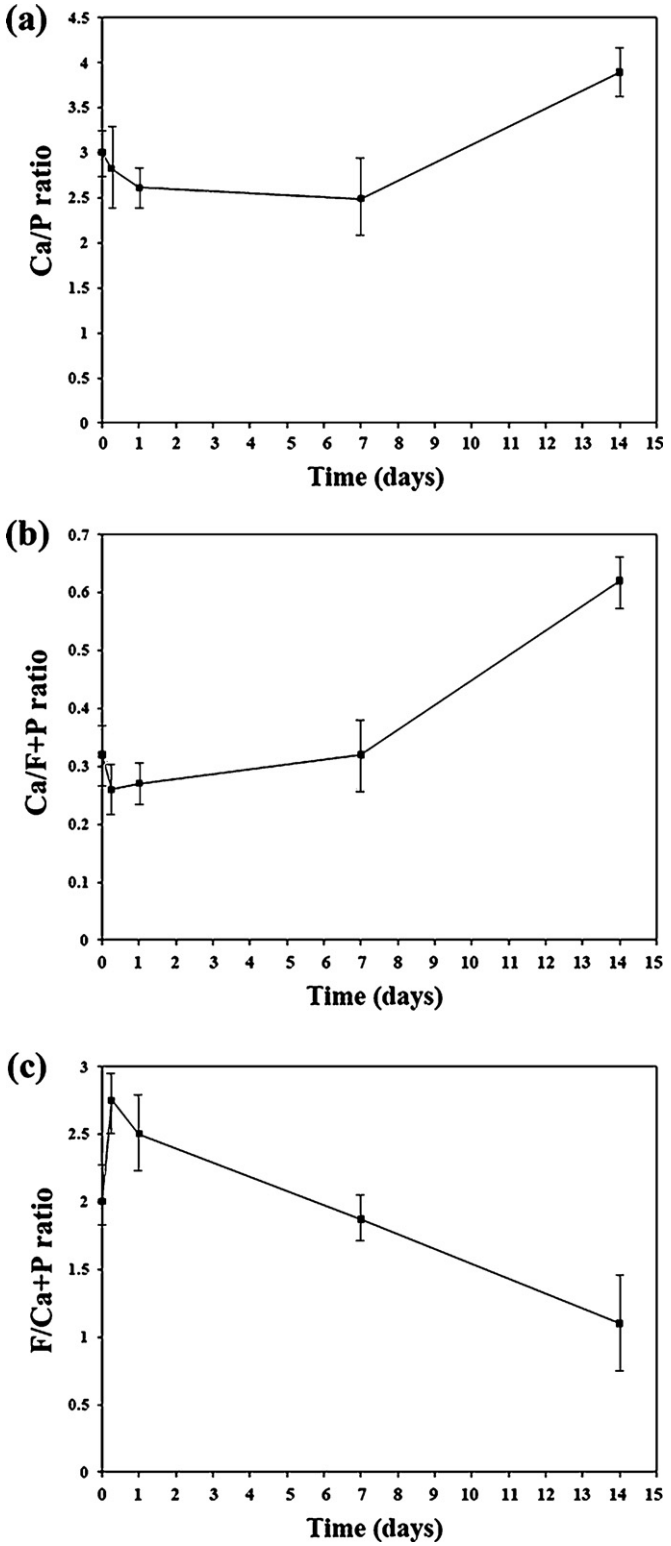

Fig. 5. Variation of different atomic ratio of biphasic powder during incubation in SBF solution, (a) Ca/P ratio, (b) Ca/(P + F), (c) F/(Ca + P).

ity[54] and stem cell response[55]. A clear relationship was shown between the size of the lattice parameter *a* and the amount of F substitution. Regarding to the obtained data from this research together with the reported results by Rodriguez-Lorenzo *et al.*, (see Table 1), it can be concluded that at least 50% of apatite solid solution phase of the synthesized sample is FAp.

3.2. FTIR analysis

Fig. 3 shows the IR spectrum obtained from the synthesized sample. The characteristic bonds and their assignments are listed in Table 2. The bond at 1033 cm^{-1} arises from ν_3 PO_4, the bonds at 608 cm^{-1} and 567 cm^{-1} arise from ν_4 PO_4. As a rule, with increasing the degree of fluorination in the structure of HAp, the intensity of peak at 605 cm^{-1} increases with respect to the peak at 565 cm^{-1}[56]. Therefore, according to the obtained results confirming that the peak at 605 cm^{-1} has more height rather than 565 cm^{-1}, substitution of OH^- groups by F^- ions in the structure of the synthesized sample can be concluded.

The minor band observed at 3445 cm^{-1} maybe due to the stretching mode of structural OH^- group in HAp while there is no band at 622 cm^{-1}, which is ascribed to librational mode of structural OH^-. Therefore, it may be concluded that the peak at 3445 cm^{-1} is most likely to be concerned with F^-. It means that most of the OH^- groups were replaced by F^- ions in the structure of apatite phase of the synthesized powder.

It is also notable that, some carbonate content was observed (CO_3^{-2} peak around 868, 1384 and 1639 cm^{-1}), which is an indication of the presence of carbonate along with fluoride in the structure of apatite, which might have originated from the absorption of carbon dioxide from the atmosphere [57,58].

3.3. Elemental analysis

To determine the exact content of each compound in the synthesized sample, elemental analysis was done, which revealed the amount of Ca and F elements in the biphasic powder. Since, Ca and F exist either in FHAp and CF, mathematical equations were drawn based on the data shown in Table 3, to evaluate the percentage of each compound in the final precipitate. Results shows that the synthesized sample includes about 46 (wt. %) of CF and 54 (wt. %) of FHAp.

3.4. In vitro bioactivity assessment in SBF solution

The SEM micrographs and related EDS data analysis of the synthesized samples before and after soaking in SBF solution at regular intervals (6 h and 1, 3, 7, 14 days) are shown in Fig. 4, which shows the surface of samples before and after soaking that can be used for comparison.

For all of the soaked biphasic powders, 50-500 nm crystallites were observed on the particle surfaces after soaking in SBF solution. Furthermore, as shown in the respective EDS analysis results, elements Ca, O, P and F were detected on the surfaces for all the soaked samples. As it can be seen in this figure, there is no distinct difference between morphology of initial synthesized powder and the samples soaked in SBF solution for various times up to 14 days.

To understand what has happened during incubation in SBF solution, the results of EDS analysis were studied precisely. For

this aim, variation of mean value for Ca/P, Ca/(P + F) and F/(Ca+P) atomic ratios was drawn versus time which is shown in Fig. 5. According to Fig. 5 (a), Ca/P ratio which was 3 for the prepared biphasic powder, decreased in the initial days and reached to 2.5 at 7th day, whereas increased sharply from 7th to 14th day up to the value 3.9. This behavior confirmed that during the first week, the synthesized powder underwent dissolution of Ca and P atoms while Ca atoms from either CF or FHAp dissolved more than P atoms from FHAp. At the second week, Ca/P ratio reached to 3.9 which is more than the initial value of the synthesized powder. This observation confirmed deposition of a new calcium/phosphate phase on the surface of samples during the second week.

Since, the synthesized powder itself contained apatite phase, distinction between initial apatite phase and newly formed apatite may not be concluded truly regarding Ca/P ratio. Therefore, variations of other ratios such as Ca/F and F/(Ca+P) were also studied.

Fig. 5 (b) displays variations of Ca/(P+F) ratio. Comparison of this diagram with Ca/P ratio diagram can reveal dissolution and deposition behavior of F atoms. If amount of F atoms on the surface could stay constant, variation of Ca/P would be the same as Ca/(P+F). Therefore, it is concluded that at least between 6th h and 7th day, F atoms experienced dissolution along with Ca and P atoms in SBF solution.

Variations of F/(Ca+P) ratio versus time is shown in Fig. 5 (c). Based on this diagram, F/(Ca+P) ratio increased in the first 6 h which indicates dissolution of Ca and P atoms, and decreased sharply until 14th day. This behavior confirmed that highest amount of dissolution of Ca and P atoms occurred during the initial 6 h and in this period of time, Ca and P atoms underwent more dissolution rather than F atoms.

Regarding all of the obtained results, it is obvious that deposition of an apatite phase occurred after 6 h of incubation in SBF solution which confirms the bioactivity of the synthesized biphasic powder. It is also important to point out, since the synthesized powder which was soaked in SBF solution contained FHAp, Ca/P ratio obtained from the surface of incubated powder was more than 2.5. Thus, these ratios cannot be considered as a criterion to determine what kind of calcium/phosphate phase was deposited on the surface during incubation but according to the obtained results indicating dissolution and adsorption of F atoms, it can be concluded that the newly formed calcium/phosphate phases contained fluorine in their structure.

4. Conclusion

In this research, a biphasic nanopowder consisted of CF and FHAp was successfully synthesized through a modified precipitation method using buffer solution. The bioactivity assay confirmed formation of a new calcium/phosphate phase right after soaking in SBF solution. This product can be considered as an osteoconductive dental filler or implant with the ability of dental carries prevention due to release of fluorine ions. Usage of buffer solution for this purpose not only can produces biphasic powder but also provides the possibility of establishment of a continuous process without manual interfere for adjusting pH of the reactor. To achieve this possibility, the amount of manually added buffer solution to the reactor during the synthesis process should be measured. If measured amount of buffer solution could be added to the phosphate solution before beginning the synthesis process, the same product would be obtained via a continuous method without needing to adjust pH of the reactor (Ca solution) medium.

References

[1] M. Jarcho, C.H. Bolen, M.B. Thomas, J. Bobick, J.F. Kay, R.M. Doremus, Hydroxyapatite synthesis and characterization in dense polycrystalline form, J. Mater. Sci. 11 (1976) 2027–2035.

[2] L. Dean-Mo, Fabrication of hydroxyapatite ceramic with controlled porosity, J. Mater. Sci. Mater. Med. 8 (1997) 227–232.

[3] K.D. Groot, Bioceramics consisting of calcium phosphate salts, Biomaterials 1 (1980) 47–50.

[4] T. Kanazawa, T. Umegaki, K. Yamashita, H. Monma, T. Hiramatsu, Effects of Additives on Sintering and Some Properties of Calcium Phosphates with Various Ca/P Ratios, J. Mater. Sci. 26 (1991) 417–422.

[5] L.L. Hench, Bioceramics: From Concept to Clinic, J. Am. Ceram. Soc. 74 (1991) 1487–1510.

[6] H. Qu, A.L. Vasiliev, M. Aindow, M. Wei, Incorporation of fluorine ions into hydroxyapatite by a pH cycling method, J. Mater. Sci. Mater. Med. 16 (2005) 447–453.

[7] J.C. Elliott, R.M. Wilson, S. Dowker, Apatite Structure, JCPDS-International Centre for Diffraction Data, Advances in X-ray Analysis 45 (2002) 172–181.

[8] J. Carsten, B. Marco, ^{19}F NMR spectroscopy of glass ceramics containing fluorapatites, Biomaterials 17 (1996) 2065–2069.

[9] Y. Sogo, A. Ito, D. Yokoyama, A. Yamazaki, R.Z. Legeros, Synthesis of fluoride-releasing carbonate apatites for bone substitutes, J. Mater. Sci. Mater. Med. 18 (2007) 1001–1007.

[10] C.H. Turner, G. Boivin, P.J. Meunier, A mathematical model for fluoride uptake by the skeleton, Calcif. Tissue . Int. 52 (1993) 130–138.

[11] F.C.M. Driessens, Relation between Apatite Solubility and Anti-cariogenic Effect of Fluoride, Nature 243 (1973) 420–421.

[12] E.C. Moren, M. Kresak, R.T. Zahradnik, Physicochemical Aspects of Fluoride-Apatite Systems Relevant to the Study of Dental Caries, Caries Res. 11 (1977) 142–171.

[13] J.D. Featherstone, R. Glena, M. Shariati, C.P. Shield, Dependence of in vitro demineralization of apatite and remineralization of dental enamel on fluoride concentration, J. Dent. Res. 69 (1990) 634–636.

[14] W. Qu, D. Zhong, P. Wu, J. Wang, B. Han, Sodium fluoride modulates caprine osteoblast proliferation and differentiation, J. Bone. Miner. Metab. 26 (2008) 328–334.

[15] J. Caverzasio, G. Palmer, J.P. Bonjour, Fluoride: Mode of Action, Bone 22 (1998) 585–589.

[16] K.H.W. Lau, D.J. Baylink, Osteoblastic tartrate-resistant acid phosphatase: its potential role in the molecular mechanism of osteogenic action of fluoride, J. Bone. Miner. Res. 18 (2003) 1897–1900.

[17] B.L. Riggs, W.M. Ofallon, A. Lane, S.F. Hodgson, H.W. Wahner, J. Muhs, E. Chao, L.J. Melton, 3rd Clinical trial of fluoride therapy in postmenopausal osteoporotic women: extended observations and additional analysis, J. Bone. Miner. Res. 92 (1994) 65–275.

[18] D. Haguenauer, V. Welch, B. Shea, P. Tugwell, J.D. Adachi, G. Wells, Fluoride for the treatment of postmenopausal osteoporotic fractures: a meta-analysis, Osteoporos. Int. 9 (2000) 727–738.

[19] N. Guanabens, J. Farrerons, P.L. Erez-Edo, A. Monegal, A. Renau, J. Carbonell, M. Roca, M. Torra, M. Pavesi, Cyclical etidronate versus sodium fluoride in established postmenopausal osteoporosis: a randomized 3 year trial, Bone 27 (2000) 123–128.

[20] G. Rølla, On the role of calcium fluoride in the cariostatic mechanism of fluoride, Acta. Odontol. Scan. 46 (1988) 341–345.

[21] F. Lagerlof, J. Ekstrand, G. Rolla, Effect of fluoride addition on ionized calcium in salivary sediment and in saliva, Scand. J. Dent. Res. 96 (1988) 399–404.
[22] G. Rølla, E. Saxegard, Critical evaluation of the composition and use of topical fluorides with emphasis on the role of calcium fluoride in caries inhibition, J. Dent. Res. 69 (1990) 80–785.
[23] E. Saxegaard, G. Rølla, Kinetics of acquisition and loss of calcium fluoride by enamel in vivo, Caries. Res. 23 (1989) 406–411.
[24] L.M. Rodriguez-Lorenzo, K.A. Gross, Encapsulation of apatite particles for improvement in bone regeneration, J. Mater. Sci:Mater. in Med. 14 (2003) 1–5.
[25] L.C. Chow, S. Takagi, Deposition of fluoride on tooth surfaces by a two-solution mouth Rinse in vitro, Caries. Res. 25 (1991) 397–401.
[26] G.L. Vogel, Y. Mao, C.M. Carey, L.C. Chow, S. Takagi, In vivo fluoride concentrations measured for 2 h after a NaF or a new two-solution rinse, J. Dent. Res. 71 (1992) 448–452.
[27] L.C. Chow, S. Takagi, C.M. Carey, B.A. Sieck, Remineralization effects of a two-solution fluoride mouthrinse: an in situ study, J. Dent. Res. 79 (2000) 991–995.
[28] L.C. Chow, S. Takagi, S. Frukhtbeyn, S. Sieck, E.E. Parry, N.S. Liao, G.E. Schumacher, M. Markovic, Remineralization effect of a low-concentration fluoride rinse in an intraoral model, Caries. Res. 36 (2002) 136–141.
[29] L.M. Rodriguez-Lorenzo, J.N. Hart, K.A. Gross, Influence of fluorine in the synthesis of apatites. Synthesis of solid solutions of hydroxyl-fluorapatite, Biomaterials. 24 (2003) 3777–3785.
[30] H. Qu, M. Wei, Synthesis and Characterization of Fluorine-Containing Hydroxyapatite by a pH-Cyclic Method, Mater. Sci. Mater. Med. 16 (2005) 129–133.
[31] G.E. Stan, J.M.F. Ferreira, Sol-gel chemical routes for preparing bioactive fluorohydroxyapatite thin films and powders, Digest Journal of Nanomaterials and Biostructures. 1 (2006) 37–42.
[32] K.A. Gross, K. Bhadang, Sintered hydroxyfluorapatite. III. Sintering of fluoroapatite and hydroxyapatite mechanical blends and the resulting mechanical properties, Biomaterials. 25 (7–8) (2004) 1395–1405.
[33] U. Partenfelder, A. Engel, C. Russel, A pyrolytic route for the formation of hydroxyapatite/fluorapatite solid solutions, J. Mater. Sci. Mater. Med. 4 (1993) 292–295.
[34] S. Fujihara, Y. Kadota, T. Kimura, Role of organic additives in the sol-gel synthesis of porous CaF2 anti-reflective coatings, Sol-Gel. Sci. Technol. 24 (2002) 147–154.
[35] L. Zhou, D. Chen, W. Luo, Y. Wang, Y. Yu, F. Liu, Transparent glass ceramic containing Er^{3+}:CaF_2 nano-crystals prepared by sol-gel method, Mater. Lett. 61 (2007) 3988–3990.
[36] B.C. Hong, K. Kawano, Syntheses of CaF_2:Eu nanoparticles and the modified reducing TCRA treatment to divalent Eu ion, Opt. Mater. 30 (2008) 952–956.
[37] G.A. Kumar, C.W. Chen, J. Ballato, R.E. Riman, Optical characterization of infrared emitting rare-earth-doped fluoride nanocrystals and their transparent nanocomposites, Chem. Mater. 19 (2007) 1523–1528.
[38] X. Zhang, Z. Quan, J. Yang, P. Yang, H. Lian, J. Lin, Solvothermal synthesis of well-dispersed MF_2 (M = Ca,Sr,Ba) nanocrystals and their optical properties, Nanotechnology 19 (2008) 5507–5603.
[39] A. Bensalah, M. Mortier, G. Patriarcheb, P. Gredin, D. Vivien, Synthesis and optical characterizations of undoped and rare-earth-doped CaF2 nanoparticles, J. Solid. State. Chem. 179 (2006) 2636–2644.
[40] P. Aubry, A. Bensalah, P. Gredin, G. Patriarche, D. Vivien, M. Mortier, Synthesis and optical characterizations of Yb-doped CaF_2 ceramics, Opt. Mater. 31 (2009) 750–753.
[41] X. Sun, U. Li, Size-controllable luminescent single crystal CaF_2 nanocubes, Chem. Commun. (2003) 1679–1768.
[42] F. Wang, X. Fan, D. Pi, M. Wang, Synthesis and luminescence behavior of Eu^{3+}-doped CaF 2 nanoparticles, Solid. State. Commun. 133 (2005) 775–779.
[43] M. Mortier, A. Bensalah, G. Dantelle, G. Patriarche, D. Vivien, Rare-earth doped oxyfluoride glass-ceramics and fluoride ceramics: Synthesis and optical properties, Opt. Mater. 29 (2007) 1263–1270.
[44] L. Wang, B. Wang, X. Wang, W. Lu, Tribological investigation of CaF2 nanocrystals as grease additives, Tribol. Int. 40 (2007) 1179–1185.
[45] R.N. Grass, W.J. Stark, Flame synthesis of calcium-, strontium-, barium fluoride nanoparticles and sodium chloride, Chem. Commun. (2005) 1767–1769.
[46] L. Sun, L.C. Chow, Preparation and properties of nano-sized calcium fluoride for dental applications, Dental. materials. 24 (2008) 111–116.
[47] K. Kokubo, S. Ito, Z.T. Huang, T. Hayashi, S. Sakka, T. Kitsugi, T. Yamamuro, Solutions able to reproduce in vivo surface-structure changes in bioactive glass– ceramics A–W, J. Biomed. Mater. Res. 24 (1990) 721–734.
[48] J. Kenkel, analytical chemistry for technician, third ed., CRC Press, USA, 2003.
[49] B.D. Cullity, S.R. Stock, Elements of X-ray diffraction, first ed., Addison-Wesley, Massachusetts, 1956.
[50] J.Y. Kim, Z. Dong, T.J. White, Model Apatite Systems for the Stabilization of Toxic Metals: II, Cation and Metalloid Substitutions in Chlorapatites, J. Am. Ceram. Soc. 88 (2005) 1253–1260.
[51] P. Nongkynrih, S. Troy, S.K. Gupta, P.V. Rao, Crystal structure of the substituted apatites –deviation from Vegard's Law, J. Mat Sci. 23 (1988) 3243–3247.
[52] K.A. Gross, L.M. Rodriguez-Lorenzo, Sintered hydroxyfluorapatites. II. Mechanical properties of solid solutions determined by microindentation, Biomaterials 25 (7–8) (2004) 1385–1394.
[53] M. Okazaki, H. Tohda, T. Yanagisawa, et al., Differences in solubility of two types of hetrogenous fluorinated hydroxyapatites, Biomaterials 19 (7–9) (1998) 611–616.
[54] H. Eslami, M. Solati-Hashjin, M. Tahriri, Effect of fluorine ion addition on structural, thermal, mechanical, solubility and biocompatibility characteristics of hydroxyapatite nanopowders, Advanced in Applied Ceramics 109 (4) (2010) 200–212.
[55] J Harrison, A. Melville, J. Forsythe, B.C. Muddle, A.O. Trounson, K.A. Gross, R. Mollard, Sintered Hydroxyfluorapatite. IV. The effect of fluoride substitution upon colonization of hydroxyapatites by mouse embryonic stem cells, Biomaterials 25 (2004) 4977–4986.
[56] A. Shemesh, Crystallinity and diagenesis of sedimentary apatites, Geochim. Cosmochim. Acta. 54 (1990) 2433–2438.
[57] M. Komath, H.K. Varma, Development of a fully injectable calcium phosphate cement for orthopedic and dental applications, Bull. Mater. Sci. 4 (2003) 415–422.
[58] M. Wei, J.H. Evans, T. Bostrom, L. Grondahl, Synthesis and Characterisation of Hydroxyapatite, Fluoride-Substituted Hydroxyapatite and Fluorapatite, J. Mater. Sci. Mater. Med. 14 (2003) 311–320.